to J). Lineage reconstruction was performed for all of the cells of the outermost layer of the SAM, the L1 layer, of Dex-treated plants (n = 3), based on images acquired at 12-hour intervals. Mock-treated plants (n = 3) and Dex-treated plants that did not carry the RNAi construct (n = 2) served as controls. As these two control genotypes showed no significant differences, the control data were pooled. Cell division activity was expressed as the size of individual lineages [the number of progeny cells at 108 hours that descended from a single cell present at 60 hours (Fig. 4M)]. Cells of Dex-treated plants had larger lineages compared with the controls, which demonstrated an increase in cell division after compromise of CLV3 function. The lineage data were represented by superimposing each lineage on a reconstruction of the L1 at the 108-hour time point (Fig. 4, K and L). This revealed that the increase in cell division rate is observed distant from the meristematic center (Fig. 4L) and, therefore, represents a long-distance effect of events that started in the CZ.

This study provides evidence that CLV3 signaling in meristems mediates both cell fate specification and growth control through inhibition of cell division rate, as well as that the processes can be temporally uncoupled. The gradual radial expansion of the CZ that follows reduction in CLV3 activity indicates a process of PZ cell respecification that either spreads from the CZ with time or reflects a gradient of response to a CZ-promoting activity. If the signal does spread with time, it could do so either by diffusion or by stepwise communication between adjoining cells. The presently proposed function of CLV3 is to confine the expression of the transcription factor WUS to a limited set of cells as a result of CLV1 activation, and this is consistent with the WUS in situ hybridization results. A real-time analysis of WUS levels and the *WUS*-expression domain in the reorganizing meristems of *CLV3*-RNAi plants should yield further insights into the relation between cell-cell communication in the SAM and its organization and growth, as should manipulations of WUS activity during live imaging. It is not yet known whether the long-range effect of CLV3 in repressing cell division is mediated through its effect on WUS activity. Earlier studies have proposed that WUS is required for CZ specification and that SHOOTMERISTEMLESS (STM), a homeodomain protein, is required for division of PZ cells (*15*). Such a model would predict that CLV-mediated growth inhibition should impinge on STM and its regulatory cascades. It will be illuminating to test the function of STM and its regulation by the CLV-WUS network in real-time experiments such as those introduced here. However, it is also possible that the increased cell division rates that follow CLV3 removal could be an indirect consequence of the influence exerted by the expanding CZ on adjacent PZ cells. Meristems with alterations in WUS and STM activity, like the experiments related here in which CLV3 activity has been manipulated, should allow the dissection of the influence of signaling between cells on cell-fate specification, organization, and growth in SAMs, despite their being highly coupled in space and in time in wild-type plants.

References and Notes

1. T. A. Steeves, I. M. Sussex, *Patterns in Plant Development* (Cambridge Univ. Press, New York, 1989).
2. E. M. Meyerowitz, *Cell* **88**, 299 (1997).
3. J. C. Fletcher, U. Brand, M. P. Running, R. Simon, E. M. Meyerowitz, *Science* **283**, 1911 (1999).
4. S. E. Clark, R. W. Williams, E. M. Meyerowitz, *Cell* **89**, 575 (1997).
5. T. Laux, K. F. Mayer, J. Berger, G. Jurgens, *Development* **122**, 87 (1996).
6. K. F. Mayer *et al.*, *Cell* **95**, 805 (1998).
7. H. Schoof *et al.*, *Cell* **100**, 635 (2000).
8. U. Brand, J. C. Fletcher, M. Hobe, E. M. Meyerowitz, R. Simon, *Science* **289**, 617 (2000).
9. S. E. Clark, M. P. Running, E. M. Meyerowitz, *Development* **119**, 397 (1993).
10. S. E. Clark, M. P. Running, E. M. Meyerowitz, *Development* **121**, 2057 (1995).
11. P. Laufs, O. Grandjean, C. Jonak, K. Kieu, J. Traas, *Plant Cell* **10**, 1375 (1998).
12. C. F. Chuang, E. M. Meyerowitz, *Proc. Natl. Acad. Sci. U.S.A.* **97**, 4985 (2000).
13. J. Craft *et al.*, *Plant J.* **41**, 899 (2005).
14. G. V. Reddy, M. G. Heisler, D. W. Ehrhardt, E. M. Meyerowitz, *Development* **131**, 4225 (2004).
15. M. Lenhard, G. Jurgens, T. Laux, *Development* **129**, 3195 (2000).

16. We thank C.-F. Chuang, I. Moore, R. Simon, and D. Ehrhardt for DNA constructs and members of the Meyerowitz laboratory for comments on the manuscript. G.V.R. was a fellow of the Jane Coffin Childs memorial fund for medical research, and this work was supported by U.S. National Science Foundation grant IOB-0211670.

Supporting Online Material
www.sciencemag.org/cgi/content/full/1116261/DC1
Materials and Methods
Figs. S1 and S2
References

17 June 2005; accepted 26 September 2005
Published online 6 October 2005;
10.1126/science.1116261
Include this information when citing this paper.

Antagonistic Actions of Ecdysone and Insulins Determine Final Size in *Drosophila*

Julien Colombani,[1*†] Laurence Bianchini,[1*] Sophie Layalle,[1*] Emilie Pondeville,[2] Chantal Dauphin-Villemant,[2] Christophe Antoniewski,[3] Clément Carré,[3] Stéphane Noselli,[1] Pierre Léopold[1‡]

All animals coordinate growth and maturation to reach their final size and shape. In insects, insulin family molecules control growth and metabolism, whereas pulses of the steroid 20-hydroxyecdysone (20E) initiate major developmental transitions. We show that 20E signaling also negatively controls animal growth rates by impeding general insulin signaling involving localization of the transcription factor dFOXO and transcription of the translation inhibitor *4E-BP*. We also demonstrate that the larval fat body, equivalent to the vertebrate liver, is a key relay element for ecdysone-dependent growth inhibition. Hence, ecdysone counteracts the growth-promoting action of insulins, thus forming a humoral regulatory loop that determines organismal size.

In metazoans, the insulin/IGF (insulin growth factor) signaling pathway (IIS) plays a key role in regulating growth and metabolism. In *Drosophila*, a family of insulin-like molecules called Dilps activates a unique insulin receptor (InR) and a conserved downstream kinase cascade that includes phosphatidylinositol 3-kinase (PI3K) and the serine-threonine protein kinase Akt [also called protein kinase B (PKB)] (*1*). Recent genetic experiments have established that this pathway integrates extrinsic signals such as nutrition with the control of tissue growth during larval stages (*2*, *3*). The larval period is critical for the control of animal growth, as it establishes the size at which maturation occurs and, consequently, the final adult size. Maturation is itself a complex process that is controlled by the steroid 20-hydroxyecdysone (20E). Peaks of 20E determine the timing of all developmental transitions, from embryo to larva, larva to pupa, and pupa to adult (*4*). Ecdysteroids are mainly produced by the prothoracic gland (PG), part of a composite endocrine tissue called the ring gland (fig. S1A).

Final adult size thus mainly depends on two parameters: the speed of growth (or growth

[1]CNRS/University of Nice–Sophia Antipolis, UMR6543, Parc Valrose, 06108 Nice Cedex 2, France. [2]CNRS FRE2852, Université P. et M. Curie, 7 quai St. Bernard, 75252 Paris, France. [3]Institut Pasteur, 25-28 rue du Docteur Roux, 75724 Paris, France.

*These authors contributed equally to this work.
†Present address: Cancer Research UK, London Institute, 44 Lincoln's Inn Fields, London WC2A 3PX, UK.
‡To whom correspondence should be addressed. E-mail: leopold@unice.fr

rate), which is primarily controlled by IIS, and the overall duration of the growth period, which is limited by the onset of the larval-pupal transition and is timed by peaks of ecdysone secretion (*5*). Little is known about the mechanisms that coordinate these two parameters during larval development (*6*).

To investigate the function of ecdysone in controlling organismal growth, we developed a genetic approach that allowed us to modulate basal levels of ecdysteroids in *Drosophila*. Our initial rationale was to modify the mass of the ring gland in order to change the level of ecdysteroid production. In pursuit of this goal, we manipulated the levels of PI3K activity in the PG by crossing *P0206-Gal4* (*P0206>*), a line with specific Gal4 expression in the PG and corpora allata (CA) (*7*, *8*), with flies carrying UAS constructs that allowed expression of either wild-type PI3K or dominant-negative PI3K ($PI3K^{DN}$). As expected, these crosses produced striking autonomous growth effects in the ring gland, and particularly in the PG: Tissue size was increased upon PI3K activation and decreased upon inhibition (Fig. 1A). Surprisingly, the changes in ring gland growth were accompanied by opposite effects at the organismal level. *P0206>PI3K* animals (with large ring glands) showed reduced growth at all stages of development and produced emerging adults with reduced size and body weight (78% of wild type; Fig. 1, A and B). Conversely, reducing PI3K activity in the ring gland of $P0206>PI3K^{DN}$ animals led to increased growth and produced adults with 17% greater weight on average (Fig. 1, A and B). Adult size increase was attributable to an increase in cell number in the wing and the eye. Adult size reduction was accompanied by a decrease in cell number in the wing and in cell size in the eye (Fig. 1B).

The timing of embryonic and larval development of these animals was comparable to that in controls. Both the L2 to L3 transition and the cessation of feeding (wandering) occurred at identical times (Fig. 1C). Moreover, animals entered pupal development at the same time, except for $P0206>PI3K^{DN}$, which showed a 1- to 2-hour delay intrinsic to the $UAS\text{-}PI3K^{DN}$ line itself. The duration of pupal development was slightly modified, however: Adult emergence was delayed in *P0206>PI3K* and advanced in $P0206>PI3K^{DN}$, albeit by less than 4 hours after 10 days of development (*9*). In contrast, the speed of larval growth was found to be increased in $P0206>PI3K^{DN}$ animals and decreased in the *P0206>PI3K* background at the earliest stage that we could measure (early L2 instar) (Fig. 1D). Because none of these effects were observed when PI3K levels were modified specifically in the CA with the use of the *Aug21-Gal4* driver (fig. S1, B and C), we can conclude that the observed phenotypes are solely due to PI3K modulation in the PG. Together, these results demonstrate that manipulating PI3K levels in the PG induces nonautonomous changes in the speed of larval growth (growth rate effects) without changing the timing of larval development.

To investigate whether these effects could be attributed to changes in 20E levels, we first measured ecdysteroid titers in third-instar larvae of the different genotypes. Early after ecdysis into third instar [74 hours after egg deposition (AED)], ecdysteroids are present at basal level; they accumulate to an intermediate plateau around 90 hours AED and reach peak levels before pupariation (120 hours AED) (*10*). Because early L3 levels are below the detection limit of our enzyme immunoassay, we measured ecdysteroid titers at the intermediate plateau (90 hours AED). In these conditions, we observed a very modest increase of ecdysteroids in *P0206>PI3K* larvae and a small but significant decrease in $P0206>PI3K^{DN}$ animals (Fig. 2A). This was further confirmed by measuring the transcript levels of a direct target of 20E, *E74B*, which responds to low and moderate levels of 20E (*11*) (Fig. 2B). However, in early L3 larvae with basal ecdysteroid levels (74 hours AED), differences in *E74B* transcripts were clearly visible, with a factor of 1.9 increase seen for *P0206>PI3K* and a factor of 1.7 decrease for $P0206>PI3K^{DN}$. These findings establish that basal circulating levels of 20E are modified in response to our manipulation of PI3K levels in the PG, and they also suggest that the observed differences in basal 20E levels equalize with the strong global increase of ecdysteroids in mid- to late L3.

Several related lines of evidence strengthen these results. First, the increase in growth rate and size observed in $P0206>PI3K^{DN}$ animals could be efficiently reversed by adding 20E to their food (Figs. 1D and 2C). Second, feeding wild-type larvae 20E recapitulated the effects observed in *P0206>PI3K* animals (Fig. 2C). Third, ubiquitous silencing of the nuclear receptor EcR by means of an inducible *EcR* RNA interference (RNAi) construct (fig. S2) resulted in a growth increase similar to that observed in $P0206>PI3K^{DN}$ larvae (Fig. 2C). Finally, the *phantom* (*phm*) and *disembodied* (*dib*) genes, which are specifically expressed in the PG and encode hydroxylases required

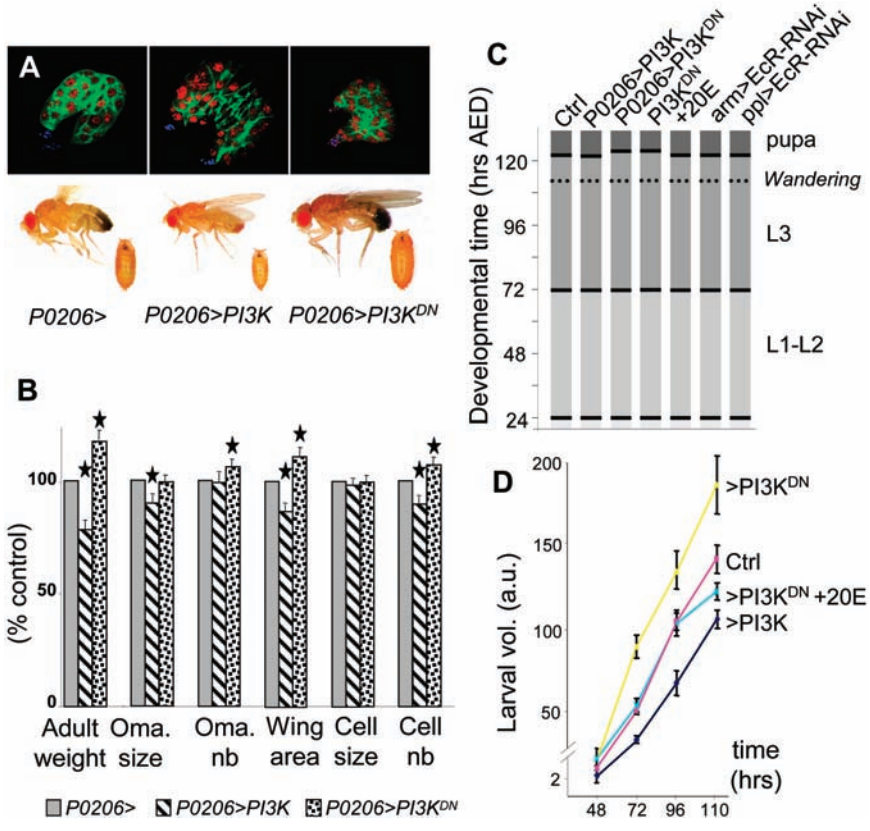

Fig. 1. Levels of PI3K signaling in the prothoracic gland control final size by changing the larval growth rate. (**A**) The *P0206-Gal4* line (*P0206>*) expresses Gal4 in the PG and the CA. Varying levels of PI3K in the ring gland produce autonomous growth effects (green, GFP; blue, anti-Elav neuronal marker; red, propidium iodide). Reverse nonautonomous growth effects are observed in pupae and adults. (**B**) Effects on body, tissue, and cell size (for weight measurement, $n = 90$; for ommatidial size, $n = 30$; for wing measurement, $n = 20$; nb, number; $^*P < 0.05$). (**C**) Timing of larval development. Transition timing (horizontal bars) is determined when 50% of the animals have passed a given transition ($n > 40$). (**D**) Measurement of larval growth rates (25°C, $n = 30$; a.u., arbitrary units). Error bars denote SD.

for ecdysteroid biosynthesis (*10*, *12*, *13*), showed increased expression (by factors of 1.65 and 2.2, respectively) upon PI3K activation in the ring gland (Fig. 2D). These results support the notion that 20E biosynthesis is mildly induced in these experimental conditions. In line with our previous results, neither 20E treatment nor EcR silencing had any effect on developmental timing (Fig. 1C). Overall, our results indicate that manipulation of basal levels of 20E signaling in various ways modifies the larval growth rate without affecting the timing of the larval transitions.

Variations in ecdysone levels in animals with different-sized ring glands could be due to changes in the PG tissue mass or, alternatively, to a specific effect of PI3K signaling in the secreting tissue. To distinguish between these two possibilities, we induced extra growth in the PG by treatment with either *Drosophila* Myc (dMyc) or cyclin D/Cdk4, two potent growth inducers in *Drosophila* (*14*, *15*). Although the size of the larval ring gland was markedly increased under these conditions (fig. S1D), no effect on pupal or adult size was observed (*9*), which implies that the size of the ring gland is not the critical factor in control of body size. Instead, it is likely that the InR-PI3K signaling pathway can specifically activate ecdysone production from the PG.

We next examined the possibility that ecdysone signaling could oppose the growth-promoting effects of IIS in the larva. To test this idea, we fed larvae 20E and assessed PI3K activity in vivo with the use of a green fluorescent protein (GFP) fused to a pleckstrin homology (PH) domain (tGPH) as a marker (*2*). Membrane tGPH localization showed a marked decrease in the fat body of 20E-fed animals, and this effect could be reversed by specifically silencing EcR in the fat body (Fig. 3A). This indicates that ecdysone-induced growth inhibition correlates with decreased IIS and is mediated through EcR. Conversely, larvae with $PI3K^{DN}$ expression in the PG showed a factor of 4.2 increase in the global levels of Akt activity, as measured by phosphorylation levels of Ser^{505} (Fig. 3B). In *Drosophila* cells (as in other metazoan cells), high levels of PI3K and Akt activity cause the transcription factor dFOXO to be retained in the cytoplasm, whereas low levels of PI3K and Akt activity allow dFOXO to enter the nucleus where it promotes *4E-BP* transcription (*16*, *17*). In larvae with ectopic *PI3K* expression in the PG, we observed a strong increase in nuclear dFOXO in fat body cells. Similar results were obtained by feeding larvae with 20E (Fig. 3C). Conversely, inactivation of EcR signaling in fat body cells was accomplished by clonal overexpression of a

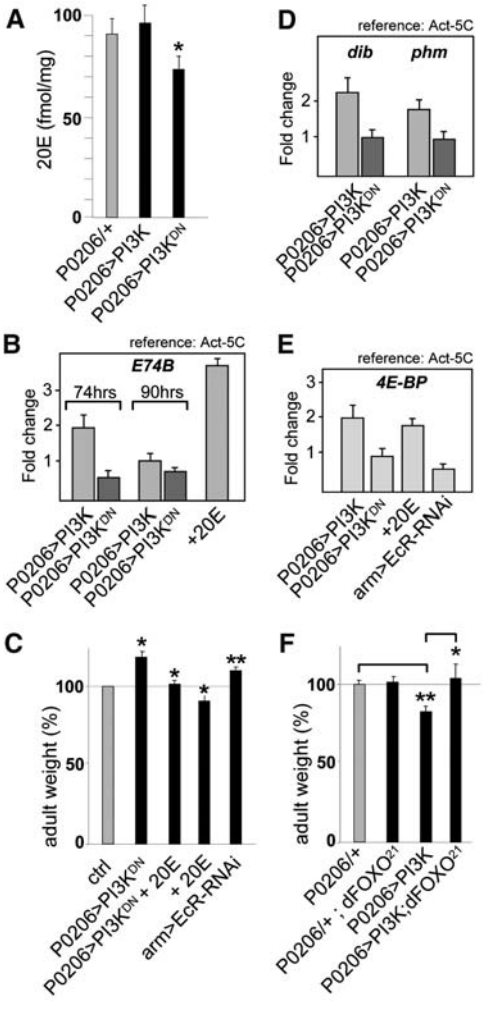

Fig. 2. 20E controls larval growth rates and final adult size. (**A**) Ecdysteroid titers in mid-L3 larvae from different genotypes (90 hours AED, $*P < 0.05$). (**B**) Measurement of larval *E74B* transcripts by quantitative reverse transcription polymerase chain reaction (RT-PCR). Fold changes are relative to control (dissection at 74 hours AED or otherwise indicated). (**C**) Effects of feeding 20E and general EcR silencing (*arm>EcR-RNAi*) on larval body weight ($*P < 0.05$, $**P < 0.01$). (**D** and **E**) Measurement of larval *dib*, *phm*, and *4E-BP* transcripts by quantitative RT-PCR. Fold changes are relative to control (dissection at 74 hours AED). (**F**) Growth defects seen in *P0206>PI3K* animals are suppressed in a $dFOXO^{21}$ homozygous background ($n > 90$, except for *P0206>PI3K; dFOXO*^{21}: $n = 60$).

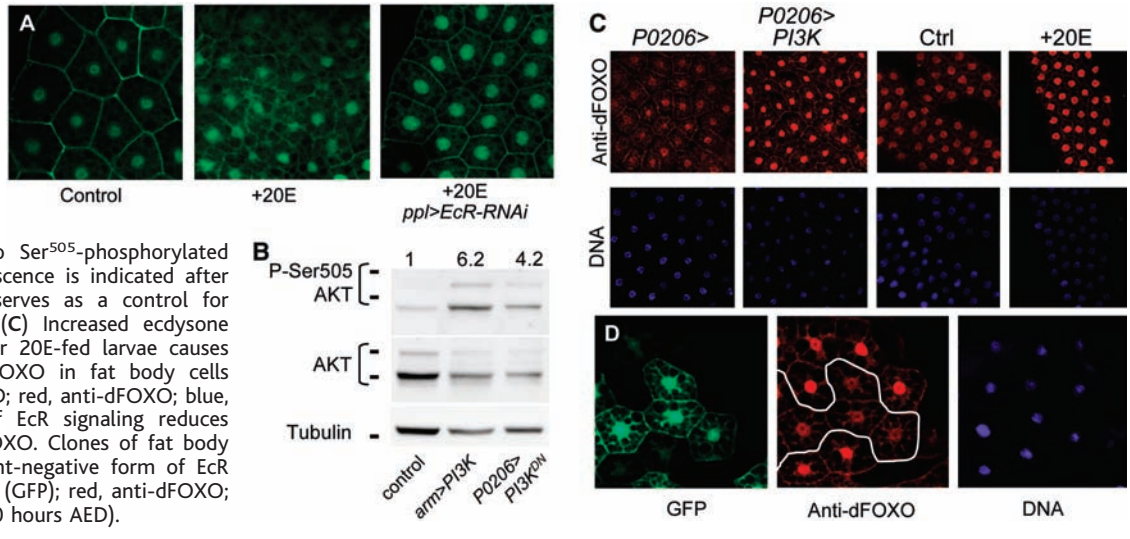

Fig. 3. Ecdysone signaling affects growth by modulating IIS. (**A**) Levels of PI3K activity in the fat body as visualized with tGPH (green) (dissection at 74 hours AED). (**B**) Global levels of activated Akt in early L3 larvae of different genotypes, detected with antibodies to Ser^{505}-phosphorylated Akt. Relative chemiluminescence is indicated after normalization. *arm>PI3K* serves as a control for increased Akt activation. (**C**) Increased ecdysone signaling in *P0206>PI3K* or 20E-fed larvae causes nuclear localization of dFOXO in fat body cells (dissection at 74 hours AED; red, anti-dFOXO; blue, DAPI). (**D**) Inactivation of EcR signaling reduces nuclear localization of dFOXO. Clones of fat body cells expressing a dominant-negative form of EcR (EcR^{F645A}) labeled in green (GFP); red, anti-dFOXO; blue, DAPI (dissection at 90 hours AED).

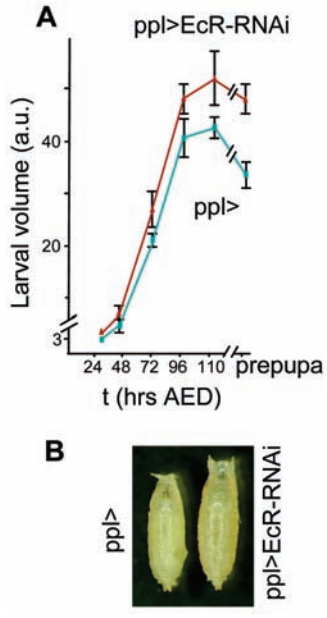

Fig. 4. The larval fat body relays the 20E-dependent growth inhibitory signal to larval tissues. The ppl-Gal4 driver (ppl>) allows specific expression of EcR-RNAi constructs in the larval fat body. (**A**) Measurement of larval volumes (n = 10 per time point). (**B**) Size difference between control and *pplGal4>EcR-RNAi* prepupae (120 hours AED).

dominant-negative form of EcR (EcR^{F645A}) (*18*). In these conditions, we observed a reduced accumulation of dFOXO in the nuclei of EcR^{F645A}-expressing cells (Fig. 3D). As an expected consequence, global accumulation of *4E-BP* transcripts was consistently higher in *P0206>PI3K* as well as in 20E-fed early L3 larvae relative to control animals, and was reduced upon general EcR silencing (*arm>EcR-RNAi*) (Fig. 2E). Together, these results indicate that ecdysone-dependent inhibition of larval growth correlates with a general alteration of insulin/IGF signaling and a relocalization of dFOXO into the cell nuclei. To more directly test the role of dFOXO in the growth-inhibitory function of ecdysone signaling, we examined the effects of increasing ecdysone levels in a *dFOXO* mutant genetic background. Although homozygous $dFOXO^{21}$ animals do not display a detectable growth phenotype (Fig. 2F) (*16*), introducing the $dFOXO^{21}$ mutation was sufficient to totally reverse the growth defects of *P0206>PI3K* animals, either homozygous (Fig. 2F) or heterozygous (*9*). These data establish that dFOXO is required for 20E-mediated growth inhibition.

The endocrine activities of the brain and the fat body have previously been implicated in the humoral control of larval growth (*19*, *20*). To test for possible roles of these two organs in mediating the systemic growth effects of ecdysone, we silenced EcR expression specifically in the brain's insulin-producing cells (IPCs) or in the fat body. Whereas specific expression of *EcR* RNAi in the IPCs failed to reproduce the overgrowth observed in *armGal4>EcR-RNAi* animals (*9*), *EcR* silencing in the fat body elicited an acceleration of larval growth and a remarkable increase in pupal size (Fig. 4, A and B). Moreover, no detectable delay was observed in the larval timing of these animals (Fig. 1C). Thus, specifically reducing 20E signaling in the fat body is sufficient to recapitulate the systemic effects of global EcR silencing. Hence, the fat body is a major target for ecdysone, and this tissue can act to relay the 20E growth-inhibitory signal to all larval tissues.

Our results establish an additional role for 20E in modulating animal growth rates. This function is mediated by an antagonistic interaction with IIS that ultimately targets dFOXO function (fig. S2E). A similar antagonistic interaction between 20E and insulin signaling was recently shown to control developmentally regulated autophagy in *Drosophila* larva (*21*).

Although we do not rule out a direct effect of ecdysone on the cellular growth rate of all larval tissues, our experiments reveal a key role for the fat body in relaying ecdysone-dependent growth control signals. Together with previous work (*3*), these data suggest that various inputs such as nutrition and ecdysone converge on this important regulatory organ, which then controls the general IIS to modulate organismal growth (fig. S2E). How, then, is growth connected to developmental timing? Our finding that 20E can modulate growth rates in addition to developmental transitions places this hormone in a central position for coordinating these two key processes and controlling organismal size.

References and Notes

1. E. Hafen, *Curr. Top. Microbiol. Immunol.* **279**, 153 (2004).
2. J. S. Britton, W. K. Lockwood, L. Li, S. M. Cohen, B. A. Edgar, *Dev. Cell* **2**, 239 (2002).
3. J. Colombani *et al.*, *Cell* **114**, 739 (2003).
4. L. M. Riddiford, *Receptor* **3**, 203 (1993).
5. H. F. Nijhout, *Dev. Biol.* **261**, 1 (2003).
6. D. Stern, *Curr. Biol.* **13**, R267 (2003).
7. G. Adam, N. Perrimon, S. Noselli, *Development* **130**, 2397 (2003).
8. W. Janning, *Semin. Cell Dev. Biol.* **8**, 469 (1997).
9. J. Colombani *et al.*, data not shown.
10. J. P. Parvy *et al.*, *Dev. Biol.* **282**, 84 (2005).
11. F. D. Karim, C. S. Thummel, *Genes Dev.* **5**, 1067 (1991).
12. V. M. Chavez *et al.*, *Development* **127**, 4115 (2000).
13. J. T. Warren *et al.*, *Insect Biochem. Mol. Biol.* **34**, 991 (2004).
14. L. A. Johnston, D. A. Prober, B. A. Edgar, R. N. Eisenman, P. Gallant, *Cell* **98**, 779 (1999).
15. D. A. Prober, B. A. Edgar, *Cell* **100**, 435 (2000).
16. M. A. Junger *et al.*, *J. Biol.* **2**, 20 (2003).
17. O. Puig, M. T. Marr, M. L. Ruhf, R. Tjian, *Genes Dev.* **17**, 2006 (2003).
18. L. Cherbas, X. Hu, I. Zhimulev, E. Belyaeva, P. Cherbas, *Development* **130**, 271 (2003).
19. E. J. Rulifson, S. K. Kim, R. Nusse, *Science* **296**, 1118 (2002).
20. T. Ikeya, M. Galic, P. Belawat, K. Nairz, E. Hafen, *Curr. Biol.* **12**, 1293 (2002).
21. T. E. Rusten *et al.*, *Dev. Cell* **7**, 179 (2004).
22. We thank G. Jarretou for technical assistance; N. Tapon, J.-P. Vincent, M. Tatar, and P. Follette for comments on the manuscript; C. Mirth and P. Caldwell for communicating unpublished results; G. Adam for discussions; and L.-E. Zaragosi and J. Hopkins for assistance with quantitative real-time fluorescence polymerase chain reaction (QPCR). Supported by CNRS, INSERM, Association pour la Recherche contre le Cancer (grants 7696 and 3339), and Fondation de France.

Supporting Online Material
www.sciencemag.org/cgi/content/full/1119432/DC1
Materials and Methods
Figs. S1 and S2
References

29 August 2005; accepted 15 September 2005
Published online 22 September 2005;
10.1126/science.1119432
Include this information when citing this paper.

Small-Molecule Inhibitor of *Vibrio cholerae* Virulence and Intestinal Colonization

Deborah T. Hung,* Elizabeth A. Shakhnovich, Emily Pierson, John J. Mekalanos

Increasing antibiotic resistance requires the development of new approaches to combating infection. Virulence gene expression in vivo represents a target for antibiotic discovery that has not yet been explored. A high-throughput, phenotypic screen was used to identify a small molecule 4-[*N*-(1,8-naphthalimide)]-*n*-butyric acid, virstatin, that inhibits virulence regulation in *Vibrio cholerae*. By inhibiting the transcriptional regulator ToxT, virstatin prevents expression of two critical *V. cholerae* virulence factors, cholera toxin and the toxin coregulated pilus. Orogastric administration of virstatin protects infant mice from intestinal colonization by *V. cholerae*.

We are entering a challenging era where microbial resistance to antibiotics will complicate the treatment of nearly all common bacterial infections. The development of antimicrobials has lagged behind the development of antibiotic resistance for many life-threatening bacterial species. Current antimicrobials, for the most part, target a relatively small number of essential gene functions, such as inhibition of cell wall synthesis, DNA replication, RNA